Resonance Energy Transfer Microscopy: Observations of Membrane-bound Fluorescent Probes in Model Membranes and in Living Cells

Paul S. Uster and Richard E. Pagano

Department of Embryology, Carnegie Institution of Washington, Baltimore, Maryland 21210. Dr. Uster's present address is Liposome Technology, Inc., Menlo Park, California 94025.

Abstract. A conventional fluorescence microscope was modified to observe the sites of resonance energy transfer (RET) between fluorescent probes in model membranes and in living cells. These modifications, and the parameters necessary to observe RET between membrane-bound fluorochromes, are detailed for a system that uses *N*-4-nitrobenzo-2-oxa-1,3-diazole (NBD) or fluorescein as the energy donor and sulforhodamine as the energy acceptor. The necessary parameters for RET in this system were first optimized using liposomes. Both quenching of the energy donor and sensitized fluorescence of the energy acceptor could be directly observed in the microscope. RET microscopy was then used in cultured fibroblasts to identify those intracellular organelles labeled by the lipid probe, *N*-SRh-decylamine (*N*-SRh-C_{10}). This was done by observing the sites of RET in cells doubly labeled with *N*-SRh-C_{10} and an NBD-labeled lipid previously shown to label the endoplasmic reticulum, mitochondria, and nuclear envelope. RET microscopy was also used in cells treated with fluorescein-labeled *Lens culinaris* agglutinin and a sulforhodamine derivative of phosphatidylcholine to examine the internalization of plasma membrane lipid and protein probes. After internalization, the fluorescent lectin resided in most, but not all of the intracellular compartments labeled by the fluorescent lipid, suggesting sorting of the membrane-bound lectin into a subset of internal compartments. We conclude that RET microscopy can colocalize different membrane-bound components at high resolution, and may be particularly useful in examining temporal and spatial changes in the distribution of fluorescent molecules in membranes of the living cell.

RESONANCE energy transfer (RET)[1] is characterized by the transfer of photon energy from one fluorochrome (the donor) to another molecule (the acceptor) that is in close physical proximity. The donor fluorescence is quenched and, if the acceptor is an appropriate fluorescent molecule, it will fluoresce as if excited directly (2). Because RET decreases in proportion to the inverse sixth power of the distance between the two probes, this phenomenon is effective only when the donor and acceptor molecules are within 100 Å of each other (31). RET therefore provides a convenient method for probing inter- and intramolecular distances in proteins (for a review, see reference 30) and in membranes. Examples of such membrane studies include those of bilayer contact (8), aggregation (11), liposome fusion (28, 38, 39), cell fusion (16), and the study of lipid–protein interactions (13, 24).

RET experiments are typically conducted in solution using a spectrofluorimeter to monitor fluorescence intensity changes at a given wavelength (3, 22, 33). Although several laboratories have made use of the improved light-gathering power of the fluorescence microscope to measure RET in specimens labeled with donor and acceptor fluorophores (7, 9, 12, 33), to our knowledge this technique has not been used as a visual microscopic tool to directly observe the sites of donor quenching and sensitized acceptor fluorescence within a specimen and to record this distribution on photographic film. Such a method would greatly enhance our ability to study the spatial distribution of fluorescent probes since the resolution of conventional light microscopy is a few tenths of a micron, while the working scale for RET is ≤100 Å.

In this paper we describe the requirements for RET to occur between fluorescent probes in model membranes, and outline the necessary modifications to a standard epifluorescence microscope for use in RET microscopy. We demon-

1. *Abbreviations used in this paper*: BHK, baby hamster kidney; (C_6-NBD)-PA, 1,2-(oleoyl, NBD-aminocaproyl) phosphatidic acid; (C_6-NBD)-PC, 1,2-(acyl, NBD-aminocaproyl) phosphatidylcholine; (C_6-SRh)-PC, 1,2-(acyl, SRh-aminocaproyl) phosphatidylcholine; (C_6-tBOC)-PC, 1,2-(acyl, *tert*-butoxycarbonyl-aminocaproyl) phosphatidylcholine; DOPC, dioleoyl phosphatidylcholine; FITC-LCA, fluorescein isothionyl-*Lens culinaris* agglutinin; HMEM, 18 mM Hepes-buffered Eagle's minimal essential medium without indicator, pH 7.4; NBD, *N*-4-nitrobenzo-2-oxa-1,3-diazole; *N*-NBD-PE, *N*-NBD-dioleoyl phosphatidylethanolamine; *N*-SRh-C_{10}, *N*-SRh-decylamine; *N*-SRh-PE, *N*-SRh-dioleoyl phosphatidylethanolamine; RET, resonance energy transfer; SRh, sulforhodamine.

strate that RET can be directly observed between fluorescent lipid analogues in model membranes and in living cells, and apply this method to study the internalization of a fluorescent lipid and lectin from the cell surface.

Materials and Methods

Dioleoyl phosphatidylcholine (DOPC), dioleoyl phosphatidylethanolamine, 1,2-(acyl, *N*-4-nitrobenzo-2-oxa-1,3-diazole-aminocaproyl) phosphatidylcholine ([C_6-NBD]-PC), *N*-NBD-dioleoyl phosphatidylethanolamine (*N*-NBD-PE), and 1,2-(oleoyl, NBD-aminocaproyl) phosphatidylcholine were purchased from Avanti Polar Lipids, Inc. (Birmingham, AL). 1,2-(Oleoyl, NBD-aminocaproyl) phosphatidic acid ([C_6-NBD]-PA) was prepared enzymatically from 1,2-(oleoyl, NBD-aminocaproyl) phosphatidylcholine as previously described (20). 1,2-(Acyl, *tert*-butoxycarbonyl-aminocaproyl) phosphatidylcholine ([C_6-tBOC]-PC) was synthesized by Avanti Polar Lipids, Inc. Fluorescein isothionyl-*Lens culinaris* agglutinin (FITC-LCA) was purchased from Vector Laboratories, Inc. (Burlingame, CA). Sulforhodamine (SRh) sulfonyl chloride (Texas Red) was purchased from Molecular Probes Inc. (Junction City, OR), and low-melting (37°C) agarose was purchased from FMC Corp. (Rockland, ME). Glass-distilled organic solvents were from Burdick and Jackson Laboratories Inc. (Muskegon, MI), and acetyl chloride was purchased from Alltech Associates, Inc. (Deerfield, IL). Decylamine, ammonium chloride, and miscellaneous reagents were purchased from Sigma Chemical Co. (St. Louis, MO). Cell culture media and supplements were purchased from Gibco (Grand Island, NY).

Phospholipid concentrations were determined by the method of Rouser et al. (26). All lipids were stored in chloroform at −70°C, periodically examined for purity, and re-purified when necessary.

Synthesis of Fluorescent Lipids

Synthesis of N-SRh-C_{10}. 1 mg of SRh sulfonyl chloride was added to 2.5 mg of decylamine in 0.5 ml of anhydrous pyridine. The mixture was allowed to react overnight under nitrogen at room temperature without stirring. Pyridine was removed by evaporation under nitrogen and the residue was extracted according to the procedure of Bligh and Dyer (5) using 0.2 M KCl/0.2 N HCl in the aqueous phase. The lower phase was washed three times with synthetic upper phase (methanol/acidic KCl buffer, 2.0:1.8), purified by thin-layer chromatography on 0.25-mm thick silica gel G plates (Merck & Co., Inc., Rahway, NJ) in chloroform/methanol/acetic acid/water (550:330:88:44) (solvent A), and extracted from the silica gel (5). *N*-SRh-C_{10} (R_f = 0.95) was recovered in 6% yield.

Synthesis of N-SRh-PE. *N*-SRh-dioleoyl phosphatidylethanolamine (*N*-SRh-PE) was synthesized essentially as previously described (29) but with the substitution of SRh sulfonyl chloride for lissamine rhodamine B sulfonyl chloride. The material was purified by thin-layer chromatography on 0.25-mm thick silica gel G plates (Merck & Co., Inc.), developed in chloroform/methanol/28% ammonium hydroxide (65:35:5) (solvent B), and extracted from the silica gel. Each of the two major products (R_f values of 0.89 and 0.93) were recovered in 17% yield. Both products were phosphate-positive, had the same mobility as SRh derivatives synthesized from a radiolabeled dioleoyl phosphatidylethanolamine precursor, and had similar SRh fluorescence spectra (λ_{ex} = 585nm, λ_{em} = 605nm) at 0.5 mol % in DOPC small unilamellar liposomes. Each is probably the product of one of the two mixed isomers of SRh sulfonyl chloride. The 0.93 isomer of *N*-SRh-PE was used exclusively in this study.

Synthesis of (C_6-SRh)-PC. (C_6-SRh)-PC was synthesized from SRh sulfonyl chloride and deblocked (C_6-tBOC)-PC. (C_6-tBOC)-PC was dried overnight under vacuum with phosphorus pentoxide as the desiccating agent. Reagent grade methanol was dried over anhydrous sodium sulfate and filtered before use. Anhydrous HCl was prepared by adding 5 ml acetyl chloride dropwise to 3 ml ice-cold methanol while stirring. The product was diluted to ~6% HCl by the addition of 45 ml glacial acetic acid. (C_6-tBOC)-PC was deblocked by dissolving 50 mg in 3.3 ml freshly prepared anhydrous 6% HCl in glacial acetic acid, and incubation at room temperature for 2 h (Struck, D. K., and R. E. Pagano, unpublished observations). 10 ml distilled water, 10 ml methanol, and 12 ml chloroform were added while vortex mixing, and the solution was neutralized by the dropwise addition of 10 N NaOH. The phases were separated, and the lower phase was washed three times with neutral synthetic upper phase. Deblocked (C_6-tBOC)-PC, identified by a decrease in thin-layer chromatographic mobility and sensitivity to phosphate- and ninhydrin-detection reagents, was purified by thin-layer chromatography in solvent A (R_f = 0.28).

2 mg of deblocked (C_6-tBOC)-PC was dried under nitrogen, resuspended in 0.5 ml of 100 mM Na_2CO_3/N,N-dimethylformamide (4:1, pH >10), and added to 2 mg SRh sulfonyl chloride. The mixture was allowed to react for 2 h at room temperature, extracted, and purified by thin-layer chromatography in solvent A. The broad band (R_f = 0.45) was scraped off the plates, extracted, and re-chromatographed in solvent A. The broad band was resolved into two products (R_f values of 0.43 and 0.52). The material at an R_f = 0.52 was scraped, extracted, and chromatographed in solvent B (R_f = 0.15). This fluorescent product, designated (C_6-SRh)-PC, was phosphate-positive and a suitable substrate for phospholipases A_2, C, and D.

Preparation of Liposomes

DOPC and fluorescent lipid were co-dissolved in ethanol and rapidly injected into 10 mM Hepes-buffered, calcium- and magnesium-free Puck's saline at pH 7.4 to produce small unilamellar liposomes of limiting radius as described by Kremer et al. (17). These liposomes were dialyzed against 18 mM Hepes-buffered Eagle's minimal essential medium without indicator, pH 7.4 (HMEM) overnight at 4°C.

Macroscopic, oligolamellar liposomes for RET microscopy were prepared by co-dissolving the fluorescent lipid of interest at 1 mol % with DOPC in chloroform. The chloroform solution was added dropwise to microscope slides or No. 1 coverslips warmed to 40°C on a thermal block. A coverslip was allowed to dry and then inverted onto a slide prepared similarly. 10 μl of 10 mM Hepes-buffered, calcium- and magnesium-free Puck's saline (pH 7.4) containing 0.4% (wt/vol) low-melting agarose was added to the side of the coverslip and the liposomes were allowed to hydrate for 30 min at 40°C. The macroscopic, hydrated lipid dispersions were immobilized for photomicroscopy by cooling the slides to room temperature and permitting the agarose matrix to solidify. The macroscopic, oligolamellar liposomes appeared transparent to slightly gray by phase-contrast microscopy.

Dispersions of 100 mol % *N*-SRh-C_{10} or (C_6-SRh)-PC were prepared by dissolving the fluorescent lipid in ethanol and rapidly injecting this solution into HMEM at a final ethanol concentration of 0.5% (vol/vol). The dispersed fluorescent lipid was then added to the culture dishes (see below).

Cell Incubation with Fluorescent Lipids

Cell Culture. Baby hamster kidney fibroblast CCL 10, BHK-21 clone 13 (baby hamster kidney) stocks were obtained from the American Type Culture Collection (Rockville, MD). Monolayer cultures were grown in Dulbecco's modified Eagle's medium (pH 7.4) supplemented with 10% heat-inactivated fetal calf serum, 10% tryptose phosphate broth, and 50 μg/ml gentamicin. Cultures were routinely grown on plastic culture dishes in an atmosphere of 5% CO_2 in air and passed by scraping. For microscopy, BHK fibroblasts were grown on acid-etched No. 1 glass coverslips. These coverslips had been boiled 30 min in 0.1 N HCl, rinsed thoroughly in deionized water, and stored in 70% ethanol before use.

Cells were washed three times with HMEM, incubated with fluorescent probes as described below, and washed three times with HMEM. For microscopy, coverslips were inverted onto depression-well slides filled with HMEM. For other analyses, cultures were extracted at 2°C with two ml of 2% Triton X-100/50 mM Hepes/1 mM EDTA buffer. Fluorescence was quantified using standards of known concentration in the same buffer. Extracted cell protein was estimated using the method of Warburg and Christian (40) after correcting for the presence of any fluorescent probes.

Fluorescent Labeling with N-SRh-C_{10}. BHK fibroblasts were incubated with 1 μg *N*-SRh-C_{10}/ml (see above) in HMEM for 8 min at 37°C, washed, and cooled to 2°C in an ice-water bath.

Fluorescent Labeling with (C_6-NBD)-PA. *N*-SRh-C_{10} labeled or unlabeled cultures were incubated for 1 h at 2°C with (C_6-NBD)-PA/DOPC (4:6) small unilamellar liposomes (100 μM total lipid), washed in HMEM, incubated at 37°C for 15 min, and returned to the 2°C ice-water bath before microscopic examination.

Fluorescent Labeling with (C_6-SRh)-PC. BHK fibroblasts were incubated with 2 μM (C_6-SRh)-PC (see above) for 30 min at 2°C, washed, and examined.

Fluorescent Labeling with FITC-LCA. Cells were incubated with 30 μg FITC-LCA/ml for 30 min at 2°C, washed, and examined.

Internalization of FITC-LCA and (C_6-SRh)-PC. Some doubly labeled cultures were warmed to 37°C for 15 min to allow internalization of lectin and lipid. (C_6-SRh)-PC was removed from the plasma membrane of BHK cells by three successive 15-min incubations at 2°C with 0.1 mM DOPC small unilamellar liposomes. Cells were incubated for 10 min in HMEM supplemented with 10 mM ammonium chloride before microscopic examination to enhance pH-sensitive fluorescence of FITC-LCA (37).

Table I. Optical Filters for RET Microscopy Using NBD or Fluorescein As the Donor, and SRh As Acceptor Fluorochromes

Channel	Zeiss filter pack components			Spectral window	
	Exciter filter	Dichroic beam splitter	Barrier filter	Excitation wavelengths	Emission wavelengths
				nm	*nm*
Donor	BP436/17	FT510	BP515-565	428–444	515–565
Acceptor	BP546/12	FT580	LP620	540–552	≥610
Transfer	BP436/17	FT510	LP620	428–444	≥610

Photomicroscopy

Photomicroscopy was carried out with a Zeiss IM-35 epifluorescence microscope using a Planapo 40/0.9 numerical aperture (NA) or 63/1.4 NA objective, and an HBO 100 mercury lamp. Electronic shutters were used to control specimen illumination by the mercury and tungsten lamps. Special filter packs were assembled to delineate three optical channels on the fluorescence microscope (Table I). These were used to monitor quenching of donor fluorescence, directly excited acceptor fluorescence, and sensitized acceptor fluorescence due to RET.

Comparisons between singly and doubly labeled cells were always made from parallel cultures in the same experiment. The excitation wavelength intensity and exposure time for a given optical channel was the same in any comparison of singly and doubly labeled cells. Black and white photomicrographs were recorded on Kodak Tri-X panatomic film and push-processed to ASA 1600 using Diafine developer. Negatives and photomicrographs were exposed and processed as identically as possible to compare the fluorescence intensities of singly versus doubly labeled cells. Color photomicrographs were recorded on Kodak Ektachrome 400 film that was push-processed to ASA 1200.

In experiments where NBD photobleaching was detected, the field of interest was focused in phase contrast without any prior fluorescence illumination, and only one fluorescence photomicrograph was recorded from each field.

Fluorescence Determinations

Fluorescence spectra and intensities were recorded using an Aminco-Bowman spectrophotofluorimeter (SLM-Aminco Inc., Urbana, IL). Fluorescein, NBD, and SRh fluorescence were quantified using fluorescent standards of known concentration.

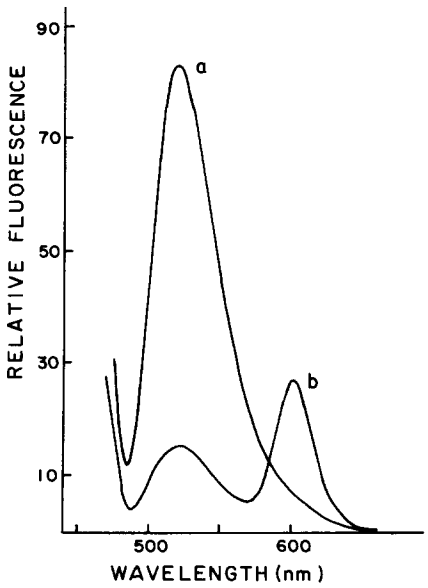

Figure 1. RET between fluorescent lipid probes in model membranes. Small unilamellar liposomes were prepared and the fluorescence emission spectra determined of: (*a*) singly labeled (DOPC/*N*-NBD-PE [99:1, mol/mol]) and (DOPC/*N*-SRh-PE [99:1]) liposomes mixed in equimolar amounts, or (*b*) doubly labeled (DOPC/*N*-NBD-PE/*N*-SRh-PE [98:1:1]) liposomes (λ_{ex} = 470 nm). Total nanomoles of *N*-NBD-PE and *N*-SRh-PE were the same in both spectra.

Results

Requirements of RET Microscopy

To use RET microscopy as a sensitive, unequivocal assay of probe co-localization, the donor fluorescence emission should overlap the absorption spectrum of the energy acceptor significantly. In addition, the fluorescent donor probe should be excited at wavelengths where the molar absorption of the acceptor probe is relatively small. This minimizes direct excitation of the acceptor and increases the fraction of acceptor probe available for energy transfer. These criteria are met by both donor/acceptor pairs used in the present study.

It has been established that the efficiency of energy transfer is proportional to the inverse sixth power of the distance of separation between donor fluorochrome and acceptor (31). For NBD and fluorescein donors, RET to energy acceptors is not appreciable beyond a 100 Å separation (35). Thus, RET between membrane-bound probes will be detected when both donor and acceptor are in the same bilayer (28, 38, 39). The emission spectrum of mixed, equimolar amounts of DOPC/*N*-NBD-PE (99:1, mol/mol) and DOPC/*N*-SRh-PE (99:1) liposomes illuminated at 470 nm demonstrates the characteristic strong NBD emission at 515–565 nm, and essentially no SRh fluorescence at 600–630 nm (Fig. 1 *a*). However, when a third population of DOPC/*N*-NBD-PE/*N*-SRh-PE (98:1:1) liposomes was illuminated, the intense green emission of NBD was quenched strongly and the fluorescence of SRh increased substantially (Fig. 1 *b*). The transferred photon energy was re-emitted at the acceptor's own characteristic emission peak as if it had been excited directly. This sensitized emission (which is indicated by the peak appearing at 600–630 nm) was concomitant with donor quenching, and is a characteristic of RET, distinguishing it from other mechanisms of fluorescence quenching (2).

The efficiency of energy transfer (E) was calculated from donor quenching using the equation

$$E = 1 - F/F_0, \quad (1)$$

where the steady-state relative fluorescence intensity is measured in the presence (F) and absence (F_0) of the acceptor (10, 13). The molar density of the membrane-bound acceptor determined the efficiency of donor fluorescence quenching (Fig. 2). Greater than 90% transfer efficiency was achieved at 1 mol % *N*-SRh-PE. The relationship of transfer efficiency to donor probe density was tested by preparing different liposome suspensions in which the molar density of *N*-NBD-PE was varied from 0.0 to 2.0 mol % at a constant *N*-SRh-PE density of 0.4 mol %. Note from Fig. 2 that at 0.4 mol %

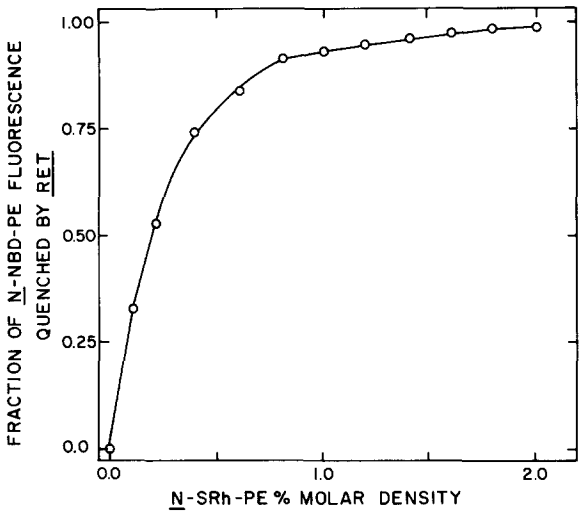

Figure 2. The molar density of the acceptor determines the transfer efficiency of membrane-bound probes. Dispersions of small unilamellar DOPC liposomes (50 μM total lipid) were prepared containing 1 mol % of the fluorescent donor N-NBD-PE, and various molar densities of *N*-SRh-PE ranging from 0.0 to 2 mol %. The transfer efficiency was calculated from Eq. 1 (see text). λ_{ex} = 435 nm; λ_{em} = 530 nm.

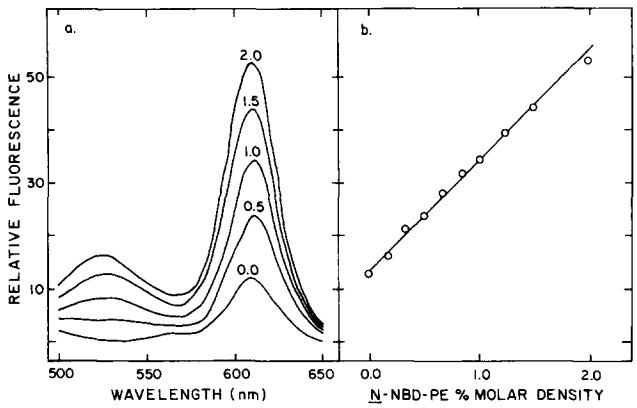

Figure 3. Sensitized acceptor fluorescence is proportional to the molar density of fluorescent donor membrane probe. DOPC liposomes (50 μM total lipid) were prepared containing 1 mol % of the fluorescent acceptor *N*-SRh-PE, and various molar densities of *N*-NBD-PE ranging from 0.0 to 2 mol %. (*a*) Each sample was excited at 435 nm, and the fluorescence emission spectra recorded for 0.0, 0.5, 1.0, 1.5, and 2.0 mol % of *N*-NBD-PE. (*b*) Plot of the fluorescence intensity at 605 nm versus donor molar density.

acceptor, the rate of change of transfer efficiency was greatest. Nevertheless, the transfer efficiency was constant (0.56 ± 0.01) over a 40-fold range of donor molar density, and also when NBD donor was in excess of the SRh acceptor density. Thus, as for other membrane-bound fluorochromes (10), the transfer efficiency was dependent on SRh probe surface density, and was independent of NBD donor surface density. In contrast, we observed that sensitized SRh acceptor fluorescence was directly proportional to the molar density of NBD donor (Fig. 3). These liposome studies suggest that to optimally record RET on film emulsion, the membranes should have an appreciable amount of acceptor probe in the bilayer to observe quenching (Fig. 2). Sensitized acceptor fluorescence must also be monitored to verify that the mechanism of quenching is due to RET, and this is best seen when the membrane is co-labeled with as great a density of fluorescent donor as is practical (Fig. 3).

Energy Transfer Microscopy of Model Membranes

We tested the ability of our modified fluorescence microscope to visually observe RET in a model membrane system (Fig. 4). The top panel of Fig. 4 schematically represents two macroscopic, hydrated, oligolamellar, DOPC liposomes. Each liposome contained 1 mol % *N*-NBD-PE, the fluorescence donor, and the liposome on the right was co-labeled with 1 mol % *N*-SRh-PE, the energy acceptor. The location of the acceptor was verified by direct excitation (λ_{ex} = 546 nm) of *N*-SRh-PE in the acceptor channel (Fig. 4, *ACCEPTOR*). If the predictions of RET can be observed visually, NBD fluorescence (λ_{em} = 515–565 nm) should be quenched in the doubly labeled liposome relative to that of the singly labeled liposome. This is precisely what was observed in the donor channel when NBD was excited directly (λ_{ex} = 436 nm, Fig. 4, *DONOR*). *N*-SRh-PE was not excited strongly at 436 nm in the absence of *N*-NBD-PE. The background in the transfer channel ($\lambda_{em} \geq 610$ nm) of liposomes singly labeled with *N*-SRh-PE was less than the background of NBD under these conditions. The background due to NBD donor in the transfer channel was detectable in the singly labeled liposome, but the sensitized emission in the doubly labeled liposome was substantial (Fig. 4, *TRANSFER*). We conclude that both donor quenching and sensitized acceptor fluorescence in model membranes can be seen directly in the fluorescence microscope with the appropriate choice of donor and acceptor fluorochromes, and microscope filter packs. Although we have used NBD and SRh as the donor and acceptor, other fluorescent lipophilic probes may be substituted with appropriate changes in the microscope filter packs.

Fluorescent Labeling of BHK Cells with SRh Probes

The results with model membranes suggested that it would be possible to visualize RET in living cells, if appropriate donor–acceptor probe pairs had overlapping but not identical intracellular membrane distributions. Therefore, SRh membrane probes were synthesized and screened for their cellular fluorescence distribution.

(C_6-SRh)-PC predominantly labeled the plasma membrane of fibroblasts incubated with this lipid at 2°C (Fig. 5 *a*). Like (C_6-NBD)-PC (27, 29), most of the (C_6-SRh)-PC was removed from the plasma membrane by incubating labeled cells with nonfluorescent liposomes (Fig. 5 *b*), suggesting that (C_6-SRh)-PC is located on the outer leaflet of the plasma membrane at 2°C.

In contrast, the SRh derivative of decylamine, *N*-SRh-C_{10}, labeled BHK cells intracellularly with only weak plasma membrane staining (Fig. 5 *d*). A lacy, intracellular meshwork, threadlike structures, and the nuclear envelope were vividly stained when BHK cells were incubated with 1 μg *N*-SRh-C_{10}/ml at 37°C for 8 min. The distribution of intracellular *N*-SRh-C_{10} staining was similar to that described for carbocyanine dyes which label the endoplasmic reticulum, mitochondria, and nuclear envelope (14, 34).

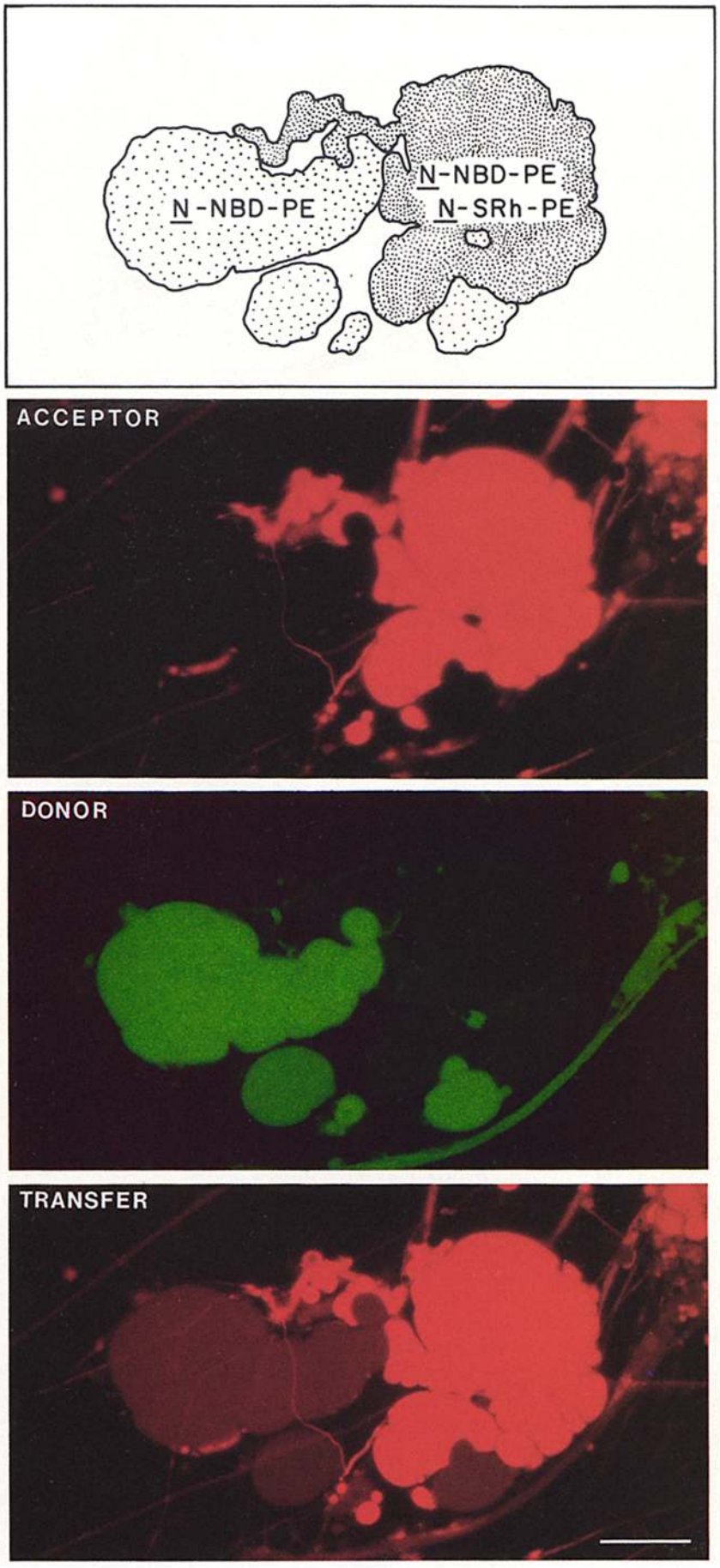

Figure 4. Energy transfer in model membranes can be visualized by energy transfer microscopy. (*Top*) Schematic representation of fluorescently labeled model membranes containing DOPC/*N*-NBD-PE (99:1, mol/mol), or DOPC/*N*-NBD-PE/*N*-SRh-PE (98:1:1). (*ACCEPTOR*) Direct excitation of SRh in the acceptor channel (λ_{ex} = 546 nm, λ_{em} ≥610 nm) verified the location of *N*-SRh-PE. (*DONOR*) Direct excitation of *N*-NBD-PE in the donor channel (λ_{ex} = 436 nm, λ_{em} = 515–565 nm). Note quenching of NBD fluorescence in the doubly labeled membranes. (*TRANSFER*) Sensitized *N*-SRh-PE fluorescence was visualized in the transfer channel (λ_{ex} = 436 nm, λ_{em} ≥ 610 nm). Some background from singly labeled model membranes was observed because NBD emits a small but detectable amount of photon energy in the red region of the visible spectrum. Bar, 20 μm.

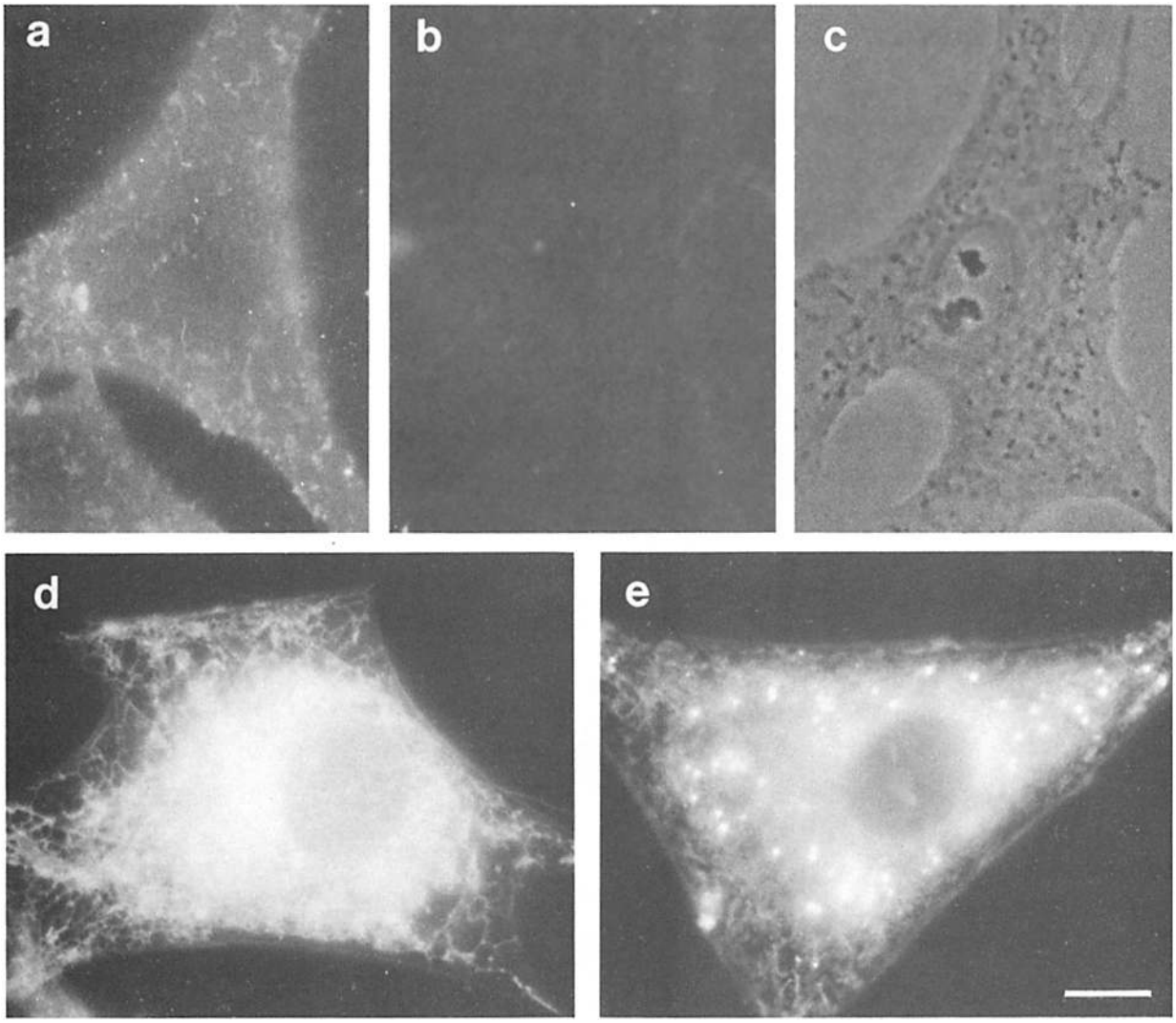

Figure 5. Cellular labeling of BHK fibroblasts with fluorescent lipophilic probes. (*a*) Cells incubated with 2 μM (C_6-SRh)-PC for 30 min at 2°C. (*b*) (C_6-SRh)-PC labeled cells after three successive incubations with 0.1 mM DOPC liposomes for 15 min at 2°C, and photographed under similar conditions as in *a*. (*c*) Phase-contrast micrograph of the field in *b*. (*d*) Cells incubated with 1 μg *N*-SRh-C_{10}/ml for 8 min at 37°C. (*e*) Cells incubated with 100 μM (C_6-NBD)-PA/DOPC (4:6) liposomes for 1 h at 2°C, washed, and warmed for 15 min at 37°C. (*a*, *b*, and *d*) Fluorescence in acceptor channel; (*e*) fluorescence in donor channel. Bar, 10 μm.

RET Microscopy between Lipophilic Probes in Living Cells

Previous work from this laboratory has demonstrated that metabolites of the acyl chain-labeled NBD analogue of phosphatidic acid, (C_6-NBD)-PA, distribute in the endoplasmic reticulum, nuclear envelope, and mitochondria of fibroblasts incubated with (C_6-NBD)-PA at 2°C (21). Intensely fluorescent lipid storage droplets become visible when the cells are warmed to 37°C (reference 20; see also Fig. 5 *e*). Thus, a detailed comparison of the intracellular membranes labeled by the metabolites of (C_6-NBD)-PA and by *N*-SRh-C_{10} was attempted using RET microscopy.

Since *N*-NBD-PE fluorescence was not photobleached significantly in model membranes, it was possible to record the same field in all three optical channels (Fig. 4). However, NBD fluorescence in living cells photobleached quickly, making it necessary to photograph different but nearby cells in each optical channel.

The endoplasmic reticulum, mitochondria, and lipid storage droplets were seen in BHK cells singly labeled with (C_6-NBD)-PA and observed in the donor channel (Fig. 6 *a*). NBD fluorescence of these intracellular compartments, with the exception of the lipid storage droplets, was markedly quenched in cells co-labeled with *N*-SRh-C_{10} (Fig. 6 *c*). This quenching was not due to reduced uptake of the NBD–lipid in doubly labeled fibroblasts (Table II).

These labeled cell cultures were examined in the transfer channel to verify the mechanism as RET (Fig. 7, *a*, *c*, and *e*). When NBD or SRh singly labeled fibroblasts were observed in the transfer channel (Fig. 7, *a* and *c*), a slight but detectable background was seen only in the perinuclear region. A comparison of *a* and *c* of Fig. 7 with the corresponding phase-contrast image indicates that the background from intracellular membranes labeled only with (C_6-NBD)-PA metabolites or *N*-SRh-C_{10} was not appreciable at the cell periphery. When fibroblasts co-labeled with both (C_6-NBD)-PA metabolites and *N*-SRh-C_{10} were observed in the

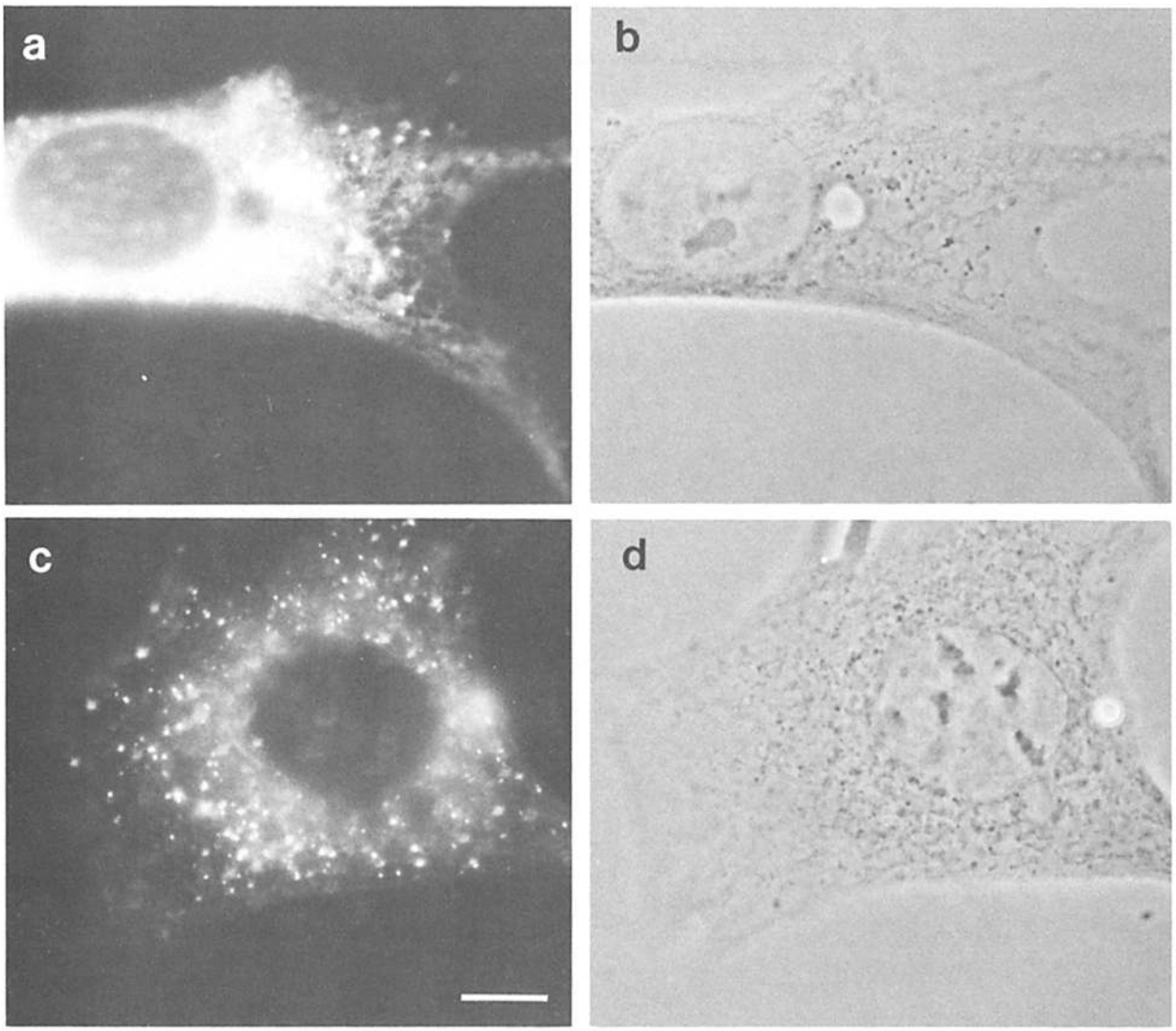

Figure 6. Donor fluorescence quenching in BHK fibroblasts labeled with (C_6-NBD)-PA and *N*-SRh-C_{10}. (*a* and *b*) Cells were incubated with 100 μM (C_6-NBD)-PA/DOPC (4:6) liposomes for 1 h at 2°C, washed, and warmed for 15 min at 37°C. (*c* and *d*) Cells were first incubated with 1 μg *N*-SRh-C_{10}/ml for 8 min at 37°C, and washed. Cells were then cooled to 2°C, and incubated with (C_6-NBD)-PA/DOPC liposomes. (*a* and *c*) Fluorescence in donor channel; (*b* and *d*) phase-contrast micrograph. Exposure time and processing for *a* and *c* were identical. Bar, 10 μm.

transfer channel, there was intense sensitized SRh emission in the endoplasmic reticulum and mitochondria (Fig. 7 *e*). The nuclear envelope was also prominently labeled, but not visible in Fig. 7 *e* because it was not in the plane of optical sectioning. Thus, donor quenching and sensitized acceptor emission between lipophilic membrane probes could be detected readily in living, intact cells.

RET Microscopy between a Fluorescently Derivatized Lectin and a Fluorescent Lipid Analogue in Cells

FITC-LCA labeled the plasma membrane of BHK cells at 2°C (Fig. 8 *a*). When fibroblasts were incubated with both FITC-LCA and (C_6-SRh)-PC there was detectable donor quenching (Fig. 8 *c*), although not as marked as that observed in lipid–lipid interactions (Fig. 6). Again, the quenching was not due to reduced lectin binding in the presence of fluorescent lipid (Table II).

There was no detectable background in the transfer channel from cells labeled only with FITC-LCA (Fig. 9 *a*), and the background from (C_6-SRh)-PC labeled fibroblasts was also negligible (Fig. 9 *c*). Thus, the sensitized (C_6-SRh)-PC fluorescence detected in the transfer channel from doubly la-

Table II. Labeling of BHK Cells by Fluorescent Probes

	nmol probe/mg cell protein*	
	Singly labeled	Doubly labeled
(C_6-NBD)-PA metabolites	9.60 ± 0.73	11.00 ± 0.93
N-SRh-C_{10}	1.15 ± 0.15	0.83 ± 0.06
FITC-LCA‡	0.24 ± 0.04	0.22 ± 0.01
(C_6-SRh)-PC	0.82 ± 0.14	0.78 ± 0.13

* Values are the mean ± SD of triplicate culture dishes.
‡ Molar concentration was calculated using 49 kD as the molecular mass of *Lens culinaris* agglutinin.

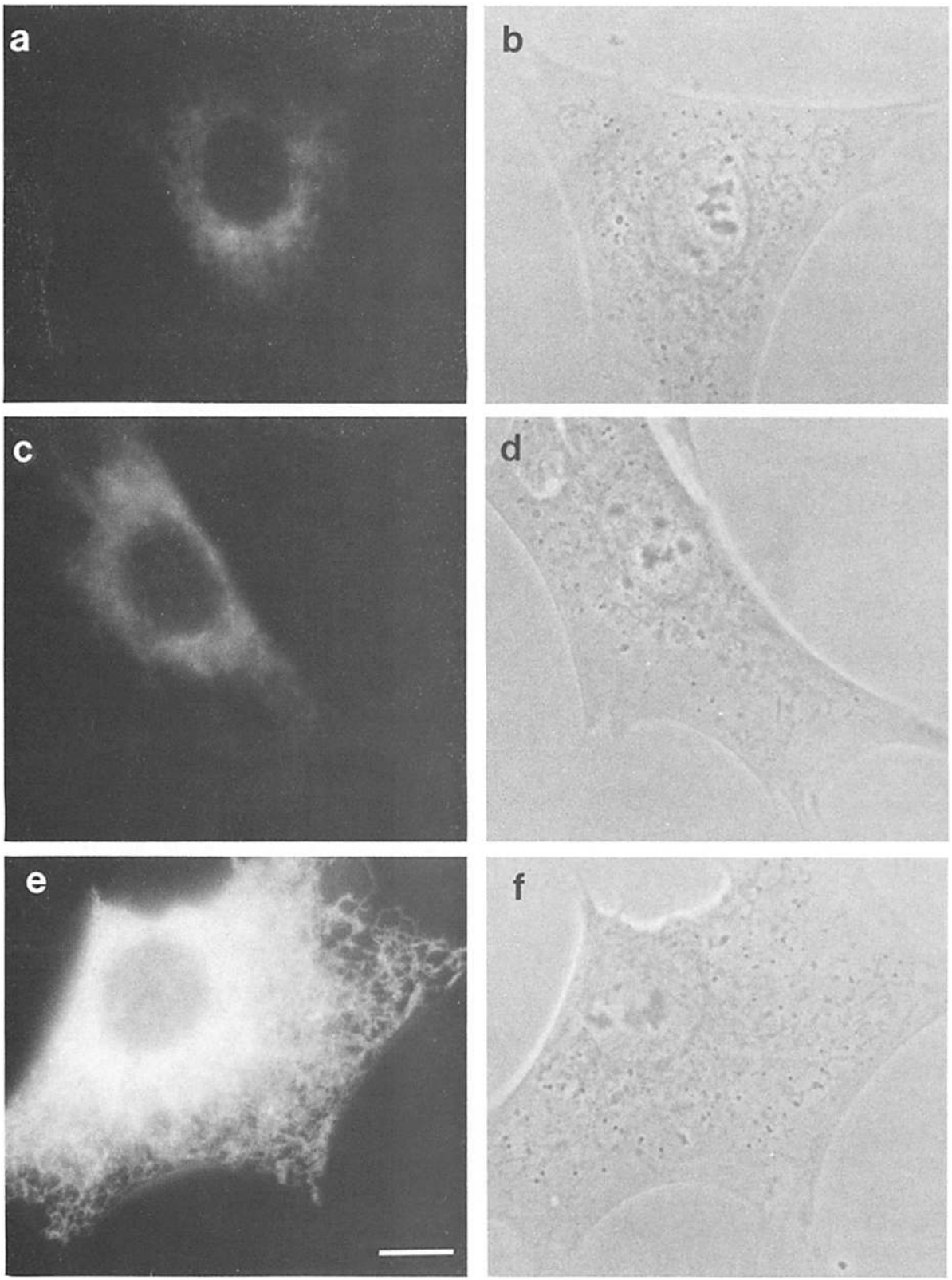

Figure 7. Sensitized acceptor fluorescence in BHK fibroblasts labeled with (C_6-NBD)-PA and *N*-SRh-C_{10}. (*a* and *b*) Cells were incubated with 100 μM (C_6-NBD)-PA/DOPC (4:6) liposomes for 1 h at 2°C, washed, and warmed for 15 min at 37°C. (*c* and *d*) Cells were incubated with 1 μg *N*-SRh-C_{10}/ml for 8 min at 37°C, and washed. (*e* and *f*) Cells were incubated as in *c* and *d*, washed, and further incubated with (C_6-NBD)-PA at 2°C. Cells were then washed and further incubated at 37°C as in *a* and *b*. (*a*, *c*, and *e*) Fluorescence in transfer channel; (*b*, *d*, and *f*) phase-contrast micrograph. Exposure time and processing for *a*, *c*, and *e* were identical. Bar, 10 μm.

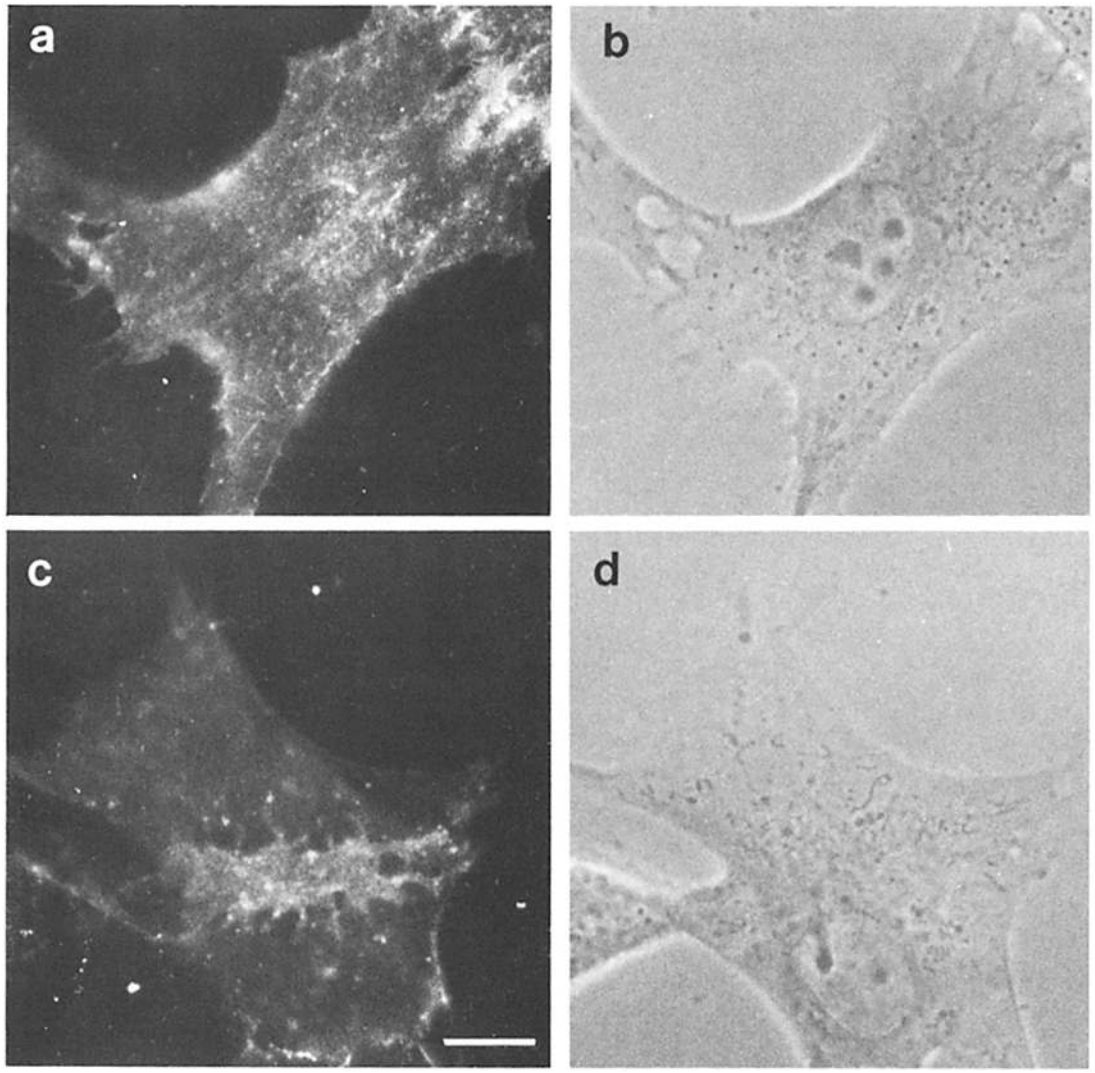

Figure 8. Donor fluorescence quenching in BHK fibroblasts labeled with FITC-LCA and (C_6-SRh)-PC. (*a* and *b*) Cells were incubated with 30 μg FITC-LCA/ml for 30 min at 2°C. (*c* and *d*) Cells were co-incubated with FITC-LCA and 2 μM (C_6-SRh)-PC for 30 min at 2°C. (*a* and *c*) Fluorescence in donor channel; (*b* and *d*) phase-contrast micrograph. Exposure time and processing for *a* and *c* were identical. Bar, 10 μm.

beled cells was due to RET (Fig. 9 *e*). The visualization of RET in the plasma membrane at 2°C under these conditions provided a positive control for internalization of these markers.

If the lectin and lipid were segregated into different compartments after internalization, it would be detected as the loss of RET, both by loss of FITC quenching and SRh sensitization. This was tested by treating BHK cells with FITC-LCA and (C_6-SRh)-PC at 2°C, and subsequently incubating at 37°C for 15 min. The cells were cooled to 2°C, and (C_6-SRh)-PC remaining at the plasma membrane was reduced with DOPC liposomes (see Materials and Methods). The cells were then incubated at 2°C in HMEM supplemented with 10 mM ammonium chloride (6, 36). This resulted in significant enhancement of internalized, pH-sensitive, FITC–lectin fluorescence by neutralizing acidic cell compartments (37).

Fig. 10 *a* indicates the fluorescence distribution of BHK cells singly labeled with (C_6-SRh)-PC after warming to 37°C and being visualized by direct excitation. Fig. 10 *b* is the same field viewed in the transfer channel, demonstrating that background from directly excited (C_6-SRh)-PC was negligible under these conditions of photomicroscopy. BHK cells singly labeled with FITC-LCA also showed no background in the transfer channel under these conditions (data not shown).

FITC-LCA fluorescence did not photobleach rapidly, and the same field of BHK cells labeled with both FITC-LCA and (C_6-SRh)-PC was photographed in all three optical channels (Fig. 11). The fluorescent lipid (Fig. 11 *b*) and fluorescent lectin (Fig. 11 *c*) were internalized to numerous intracellular vesicles. Inspection of the field revealed that the majority of internalized FITC-LCA and (C_6-SRh)-PC fluorescence co-localized in vesicles detectable in both the acceptor (Fig. 11 *b*), donor (Fig. 11 *c*), and transfer channels (Fig. 11 *d*). As in doubly labeled fibroblasts at 2°C, enhancement of (C_6-SRh)-PC fluorescence in the transfer channel due to the close proximity of fluorescent lectin was above background levels, providing evidence that fluorescent lipid and lectin were co-internalized. FITC-LCA fluorescence

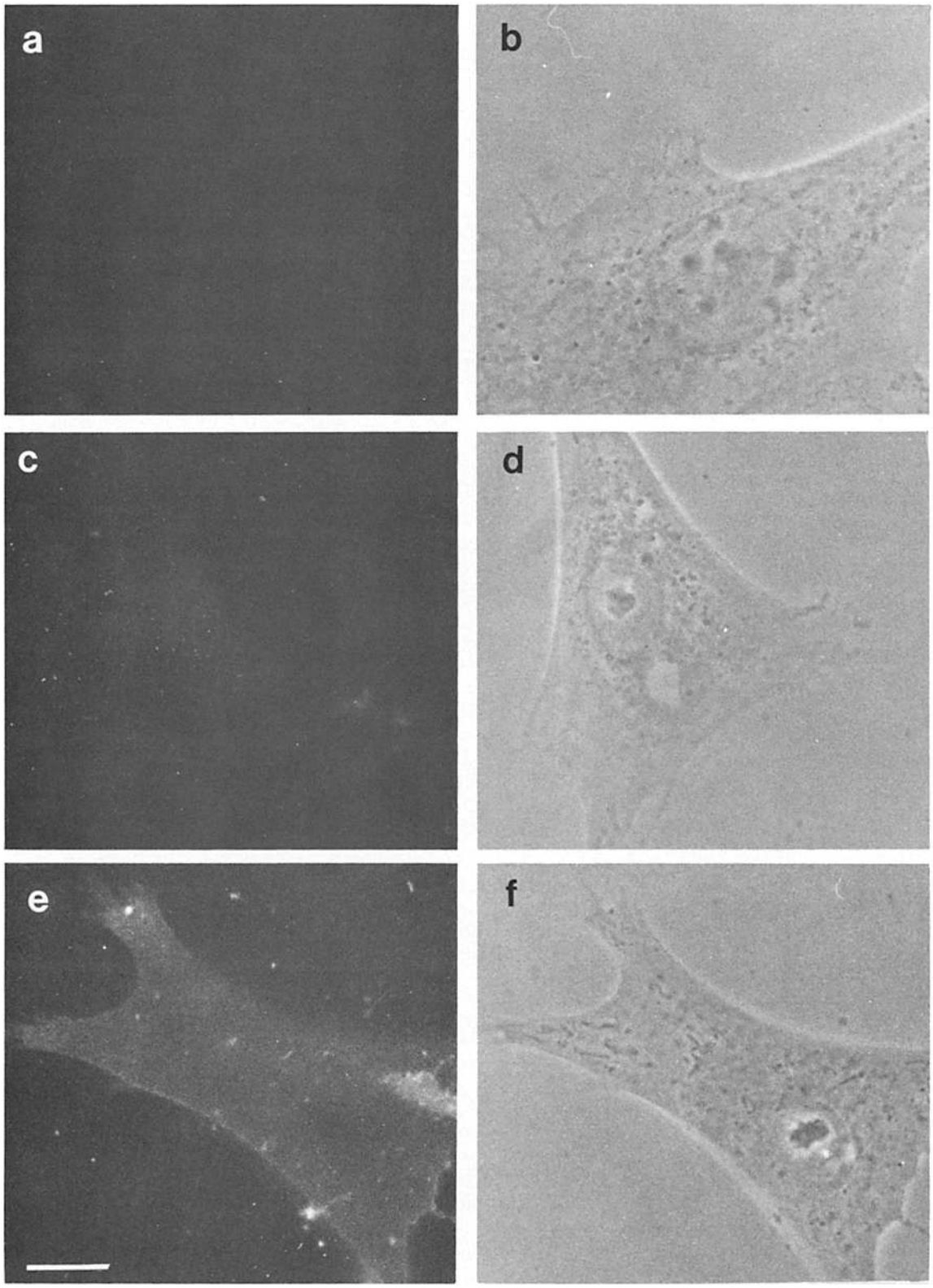

Figure 9. Sensitized acceptor fluorescence in BHK cells labeled with FITC-LCA and (C_6-SRh)-PC. (*a* and *b*) Cells were incubated with 30 μg FITC-LCA/ml for 30 min at 2°C. (*c* and *d*) Cells incubated with 2 μM (C_6-SRh)-PC for 30 min at 2°C. (*e* and *f*) Cells were co-incubated with FITC-LCA and 2 μM (C_6-SRh)-PC for 30 min at 2°C. (*a*, *c*, and *e*) Fluorescence in transfer channel; (*b*, *d*, and *f*) phase-contrast micrograph. Exposure time and processing for *a*, *c*, and *e* were identical. Bar, 10 μm.

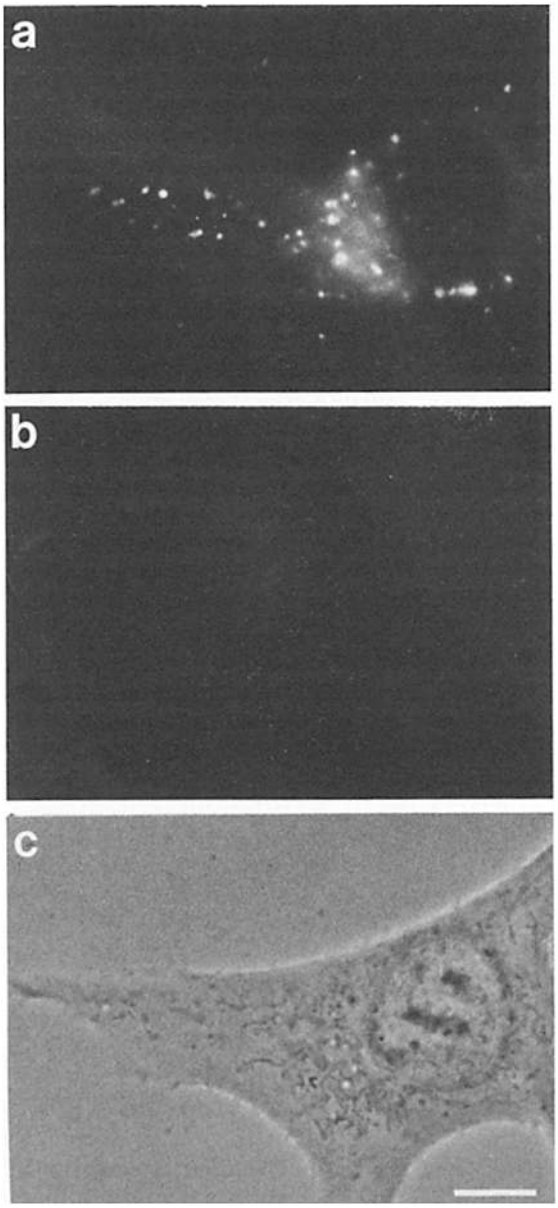

Figure 10. Internalization of (C_6-SRh)-PC in BHK fibroblasts. Cells were incubated with 2 μM (C_6-SRh)-PC for 30 min at 2°C, washed, and warmed to 37°C for 15 min. (C_6-SRh)-PC fluorescence remaining at the plasma membrane was then reduced by three incubations with DOPC liposomes at 2°C (see Materials and Methods). The same field was photographed in the (*a*) acceptor channel, (*b*) transfer channel, and by (*c*) phase contrast. Bar, 10 μm.

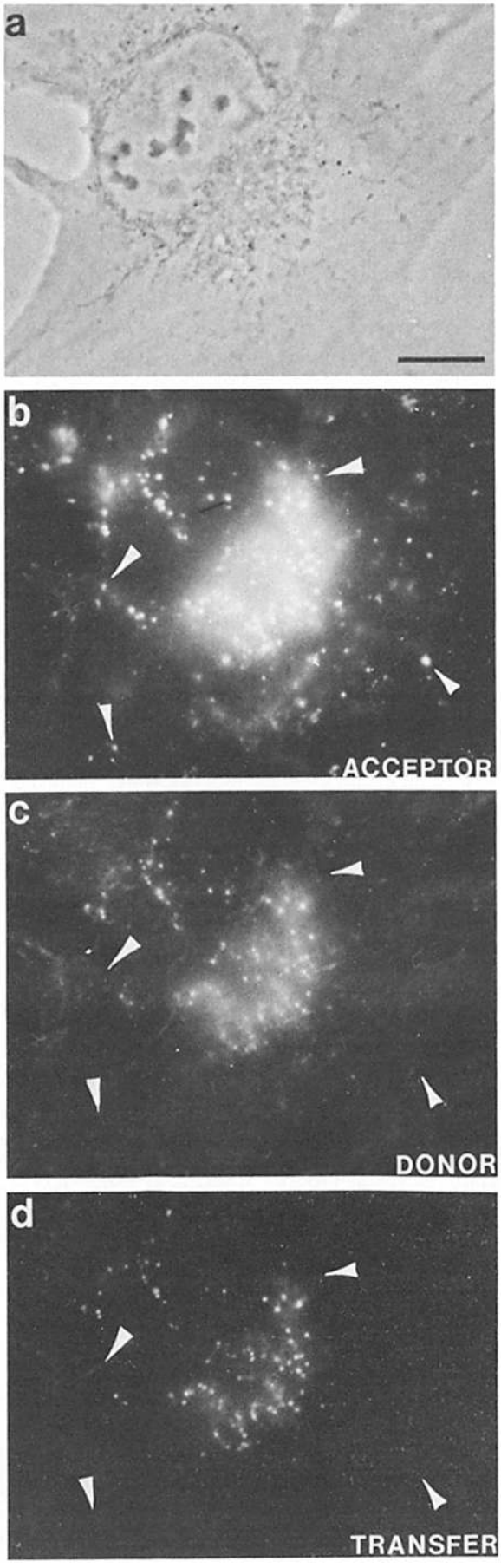

Figure 11. Internalization of FITC-LCA and (C_6-SRh)-PC in BHK fibroblasts. Cells were incubated with 30 μg FITC-LCA/ml and 2 μM (C_6-SRh)-PC for 30 min at 2°C, washed, and warmed to 37°C for 15 min. (C_6-SRh)-PC fluorescence remaining at the plasma membrane was then reduced by three incubations with DOPC liposomes at 2°C (see Materials and Methods). The same field was photographed by (*a*) phase contrast, and in the (*b*) acceptor channel, (*c*) donor channel, and (*d*) transfer channel. Exposure time and processing for Figs. 10 *b* and 11 *d* were identical. Bar, 10 μm.

quenching in doubly labeled cells was too subtle to be observed photomicroscopically when compared with singly labeled cells. However, internal punctate FITC-LCA fluorescence seen in the donor channel (Fig. 11 *c*) co-localized with sensitized (C_6-SRh)-PC fluorescence seen in the transfer channel (Fig. 11 *d*). Some vesicles containing fluorescent (C_6-SRh)-PC observed in the acceptor channel (Fig. 11 *b*, arrows) were not seen in the donor (Fig. 11 *c*, arrows) and transfer channel (Fig. 11 *d*, arrows), suggesting the absence of appreciable quantities of FITC-LCA. These results suggest that fluorescent lectin was sorted into a subset of the internal compartments labeled by (C_6-SRh)-PC.

Discussion

RET increases the usefulness of the fluorescence microscope by providing a visual method of determining if two different, fluorescently labeled membrane probes reside in the same bilayer, or if they are in physically adjacent (0.01–0.4 μm) but separate membranes. Until now, such questions have required the use of electron microscopy. Furthermore, spatial and temporal changes in the distribution of membrane probes can be followed in living cells with RET microscopy.

In this paper, we have outlined the parameters necessary to observe RET visually with membrane-bound probes in a model membrane system and extended this approach to living cells. We have constructed an optical system in which the intracellular location of two membrane probes can be correlated with changes in fluorescence intensity at the donor and acceptor emission peaks. The fluorochrome pairs and optical filter combinations maximize sensitivity while minimizing background fluorescence due to overlap of donor and acceptor probe emission spectra. Background can be reduced by selecting appropriate fluorochrome pairs, as well as by selecting the location and width of the emission window in the donor and transfer channels.

Since RET between fluorescent probes located in intracellular membranes of living cells has not been previously demonstrated, we examined the feasibility of RET in a biological system by setting up a system analogous to that of the model membranes. Namely, we doubly labeled some intracellular structures with suitable NBD and SRh probes, while retaining some compartment within the same cell labeled only with the NBD donor probe. In this study, we used RET between *N*-SRh-C_{10} and (C_6-NBD)-PA to show that *N*-SRh-C_{10} labels the endoplasmic reticulum, mitochondria, and the nuclear envelope. The fluorescence of NBD lipids in these doubly labeled organelles was markedly quenched (Fig. 6 *c*), because of the proximity of both probes in the same bilayer. When the doubly labeled cells were examined in the transfer channel and compared to the background fluorescence from singly labeled fibroblasts, just the opposite was seen (Fig. 7 *e*). Only those membranes in which both donor and acceptor probe were present could be visualized.

When doubly labeled BHK fibroblasts were examined in the donor channel, NBD-labeled lipid droplets were clearly distinguished because of quenching of NBD fluorescence in other organelles. Thus, RET microscopy could isolate a fluorescent probe in selected compartments that might otherwise be obscured by a background of interfering fluorescence.

Photobleaching of NBD lipids in living cells did not allow repeated exposures of the same cell, necessitating photography of a given cell in either the donor or transfer channel, but not both. Photobleaching is a potentially severe problem during continuous monitoring of specimens, but can be overcome with the use of low light level detector technology which operates at greatly attenuated excitation intensities (for reviews, see references 1 and 25), and by frame-summing algorithms coupled with digitized image analysis (4, 7, 15, 23). The use of fluorescence-intensity channel ratios (9, 12) and ratio-imaging digitized analysis (7, 32, 33) should also prove invaluable in those situations where photobleaching is especially severe or probe concentrations change very rapidly.

We explored the general applicability of RET microscopy by studying the internalization of a fluorescent lectin, FITC-LCA, and a new fluorescent analogue of phosphatidylcholine, (C_6-SRh)-PC. Previous observations showed that when rhodamine-labeled *Lens culinaris* agglutinin and (C_6-NBD)-PC were co-incubated in Chinese hamster lung fibroblasts, the distribution of internalized probes was not identical (27). However, initial experiments using rhodamine-labeled lectin and (C_6-NBD)-PC did not detect qualitative donor quenching and acceptor sensitization (data not shown), possibly due to the requirement for a critical surface density of the acceptor fluorochrome (see Fig. 2 for data in liposomes). Since the efficiency of RET is independent of donor surface density, the converse experiment using donor-labeled lectin and acceptor-labeled lipid was attempted.

FITC-LCA donor quenching (Fig. 8) and sensitized (C_6-SRh)-PC fluorescence (Fig. 9) occurred at the plasma membrane of BHK cells in the presence of both fluorochromes at 2°C. Fluorescence quenching was not as substantial as that between donor–lipid/acceptor–lipid pairs, and may be due to the location of the fluorescent lectin on the cell surface glycocalyx. The increased distance of separation between donor and acceptor would lead to a decrease in transfer efficiency relative to that observed for lipophilic donor/acceptor fluorochromes. The binding location of the fluorescent ligand may be an important factor, since observations in V79 cells showed no detectable FITC-LCA quenching or sensitized (C_6-SRh)-PC fluorescence under similar experimental conditions (data not shown).

Internalization of both probes should be seen in the transfer channel, and sorting into different intracellular compartments should result in the loss of RET. We envisioned four possible distributions of fluorescence (Fig. 12). (*a*) Membrane compartments would contain both the fluorescent lectin and lipid. This would be seen as sensitized (C_6-SRh)-PC fluorescence in the transfer channel that would co-localize with fluorescence in the donor and acceptor channels. (*b*) FITC-LCA and (C_6-SRh)-PC would enter the same internal compartment with loss of FITC-LCA binding or substantial dilution of the (C_6-SRh)-PC probe's surface density so that RET could not occur. This would be indicated by donor fluorescence whose pattern matched that observed in the acceptor channel, but no enhanced (C_6-SRh)-PC fluorescence in the transfer channel. (*c*) Fluorescent lipid would be visible in compartments in which there was no detectable fluorescent lectin. This would be observed as internal compartments which were visible in the acceptor channel, but not in the transfer and donor channels. (*d*) Fluorescent lectin would be visible in compartments in which there was no de-

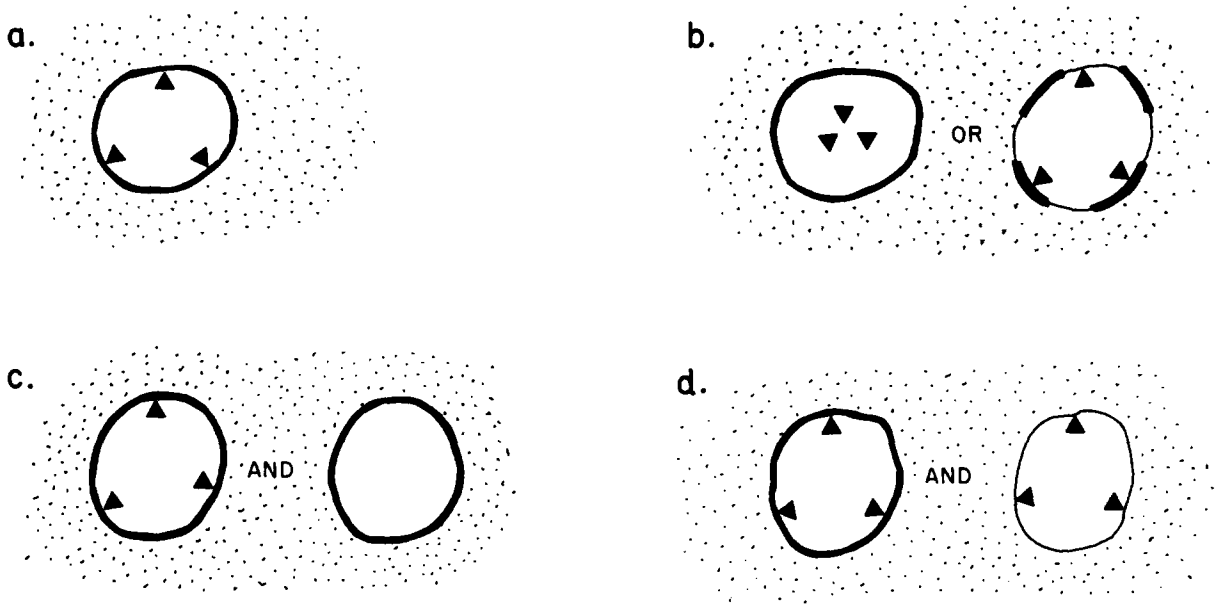

Figure 12. Possible patterns of fluorescent lectin and lipid labels within intracellular vesicles after internalization from the plasma membrane. (*a*) Lectin and lipid internalized into the same intracellular compartment without appreciable dilution of probes. (*b*) Lectin and lipid internalized into the same compartment with loss of lectin binding, or dilution of lipid probe in the membrane. (*c*) Lectin enters a subset of lipid-labeled compartments. (*d*) Lipid enters a subset of lectin-labeled compartments. See Discussion for details. (▲) FITC-LCA; (▬) (C_6-SRh)-PC labeled membranes; (———) nonfluorescent cell membranes.

tectable fluorescent lipid. This compartment would be visible in the donor channel, but not the transfer and acceptor channels.

The first and third alternatives were observed, suggesting that FITC-LCA and (C_6-SRh)-PC were co-internalized from the plasma membrane. It may be possible that changes in the surface density of either probe occurred, but our present system could not detect subtle quantitative changes. FITC-LCA appeared in a subset of the internal membrane compartments labeled by (C_6-SRh)-PC (Fig. 11), suggesting that the fluorescent lectin was sorted into certain intracellular locations, while (C_6-SRh)-PC appeared to act as a membrane marker during the internalization process. In the future, we will attempt to determine if FITC-LCA sorting occurs at the plasma membrane, or in an internal compartment.

In addition, RET microscopy will be capable of making detailed kinetic measurements of fluorescent membrane probe movement in living, intact cells when coupled with low light level detector technology and digitized image analysis. Fig. 3 suggests that quantitative measurements in the transfer channel can be monitored because enhanced SRh fluorescence is directly proportional to the molar density of the NBD lipid analogue in the same bilayer. In fact, sensitized acceptor fluorescence has been used to measure transbilayer movement and kinetic rates of NBD lipid analogue transfer between liposomes (18, 19). Initial experiments in BHK cells are consistent with our observations in model membranes, but accurate quantification will depend on image analysis.

Finally, it should be possible to study the intracellular movement and fate of micro-injected, fluorescent doubly labeled liposomes by monitoring the loss of RET if the probes are diluted into a pool of unlabeled cellular membranes (28).

The authors thank Ms. O. Martin, Messrs. M. Koval and T. Ting, and Dr. M. Edidin for critically reading the manuscript.

This work was supported by U.S. Public Health Service Grant GM-22942. P. S. Uster was a fellow of the Carnegie Institution of Washington.

Received for publication 20 March 1986, and in revised form 5 June 1986.

References

1. Arndt-Jovin, D. J., M. Robert-Nicoud, S. J. Kaufman, and T. M. Jovin. 1985. Fluorescence digital imaging microscopy in cell biology. *Science (Wash. DC).* 230:247–256.

2. Badley, R. A. 1976. Fluorescent probing of biological membranes. *In* Modern Fluorescence Spectroscopy. Vol. 2. E. L. Wehry, editor. Plenum Publishing Corp., New York. 91–168.

3. Becker, J. S., J. M. Oliver, and R. D. Berlin. 1975. Fluorescence techniques for following interactions of microtubule subunits and membranes. *Nature (Lond.).* 254:152–154.

4. Benson, D. M., J. Bryan, A. L. Plant, A. M. Gotto Jr., and L. C. Smith. 1985. Digital imaging fluorescence microscopy: spatial heterogeneity of photobleaching rate constants in individual cells. *J. Cell Biol.* 100:1309–1323.

5. Bligh, E. J., and W. J. Dyer. 1959. A rapid method of total lipid extraction and purification. *Can. J. Biochem. Physiol.* 37:911–917.

6. Ciechanover, A., A. L. Schwartz, A. Dautry-Varsat, and H. F. Lodish. 1983. Kinetics of internalization and recycling of transferrin and the transferrin receptor in a human hepatoma cell line. *J. Biol. Chem.* 258:9681–9689.

7. DiGuiseppi, J., R. Inman, A. Ishihara, K. Jacobson, and B. Herman. 1985. Applications of digitized fluorescence microscopy to problems in cell biology. *Biotechniques.* 3:394–403.

8. Ellens, H., J. Bentz, and F. C. Szoka. 1985. H^+- and Ca^{2+}-induced fusion and destabilization of liposomes. *Biochemistry.* 24:3099–3106.

9. Fernandez, S. M., and R. D. Berlin. 1976. Cell surface distribution of lectin receptors determined by resonance energy transfer. *Nature (Lond.).* 264:411–415.

10. Fung, B. K-.K., and L. Stryer. 1978. Surface density determination in membranes by fluorescence energy transfer. *Biochemistry.* 17:5241–5248.

11. Gibson, G. A., and L. M. Loew. 1979. Application of Forster resonance energy transfer to interactions between cell or lipid vesicle surfaces. *Biochem. Biophys. Res. Commun.* 88:141–146.

12. Herman, B., and S. M. Fernandez. 1982. Dynamics and topographical distribution of surface glycoproteins during myoblast fusion: a resonance energy transfer study. *Biochemistry.* 21:3275–3283.

13. Johnson, D. A., J. G. Voet, and P. Taylor. 1984. Fluorescence energy transfer between cobra α-toxin molecules bound to the acetylcholine receptor. *J. Biol. Chem.* 259:5717–5725.

14. Johnson, L. V., M. L. Walsh, B. J. Bockus, and L. B. Chen. 1981. Monitoring of relative mitochondrial membrane potential in living cells by fluorescence microscopy. *J. Cell Biol.* 88:526–535.

15. Kapitza, H. G., G. McGregor, and K. A. Jacobson. 1985. Direct mea-

surement of lateral transport in membranes by using time-resolved spatial photometry. *Proc. Natl. Acad. Sci. USA.* 82:4122–4126.

16. Keller, P. M., S. Person, and W. Snipes. 1977. A fluorescence enhancement assay for cell fusion. *J. Cell Sci.* 28:167–177.

17. Kremer, J. M. H., M. W. J. v. d. Esker, C. Pathmamanoharan, and P. H. Wiersema. 1977. Vesicles of variable diameter prepared by a modified injection method. *Biochemistry.* 17:3932–3935.

18. Nichols, J. W., and R. E. Pagano. 1982. Use of resonance energy transfer to study the kinetics of amphiphile transfer between vesicles. *Biochemistry.* 21:1721–1726.

19. Pagano, R. E., and K. J. Longmuir. 1985. Phosphorylation, transbilayer movement, and facilitated intracellular transport of diacylglycerol are involved in the uptake of a fluorescent analog of phosphatidic acid by cultured fibroblasts. *J. Biol. Chem.* 260:1909–1916.

20. Pagano, R. E., K. J. Longmuir, and O. C. Martin. 1983. Intracellular translocation and metabolism of a fluorescent phosphatidic acid analogue in cultured fibroblasts. *J. Biol. Chem.* 258:2034–2040.

21. Pagano, R. E., K. J. Longmuir, O. C. Martin, and D. K. Struck. 1981. Metabolism and intracellular localization of a fluorescently labeled intermediate in lipid biosynthesis within cultured fibroblasts. *J. Cell Biol.* 91:872–877.

22. Pardee, J. D., P. A. Simpson, L. Stryer, and J. A. Spudich. 1982. Actin filaments undergo limited subunit exchange in physiological salt conditions. *J. Cell Biol.* 94:316–324.

23. Plant, A. L., D. M. Benson, and L. C. Smith. 1985. Cellular uptake and intracellular localization of benzo(a)pyrene by digital fluorescence imaging microscopy. *J. Cell Biol.* 100:1295–1308.

24. Rehorek, M., N. A. Dencher, and M. P. Heyn. 1985. Long range lipid-protein interactions. Evidence from time-resolved fluorescence depolarization and energy-transfer experiments with bacteriorhodopsin-dimyristoylphosphatidylcholine vesicles. *Biochemistry.* 24:5980–5988.

25. Reynolds, G. T., and D. L. Taylor. 1980. Image intensification applied to light microscopy. *Bioscience.* 30:586–592.

26. Rouser, B., A. Siakotos, and S. Fleischer. 1966. Quantitative analysis of phospholipids by thin-layer chromatography and phosphorus analysis of spots. *Lipids.* 1:85–86.

27. Sleight, R. G., and R. E. Pagano. 1984. Transport of a fluorescent phosphatidylcholine analog from the plasma membrane to the Golgi apparatus. *J. Cell Biol.* 99:742–751.

28. Struck, D. K., D. Hoekstra, and R. E. Pagano. 1981. Use of resonance energy transfer to monitor liposome fusion. *Biochemistry.* 20:4093–4099.

29. Struck, D. K., and R. E. Pagano. 1980. Insertion of fluorescent phospholipids into the plasma membrane of a mammalian cell. *J. Biol. Chem.* 255:5404–5410.

30. Stryer, L. 1978. Fluorescence energy transfer as a spectroscopic ruler. *Annu. Rev. Biochem.* 47:819–846.

31. Stryer, L., and R. P. Haugland. 1967. Energy transfer: a spectroscopic ruler. *Proc. Natl. Acad. Sci. USA.* 58:719–726.

32. Tanasugarn, L., P. McNeil, G. T. Reynolds, and D. L. Taylor. 1984. Microspectrofluorometry by digital image processing: measurement of cytoplasmic pH. *J. Cell Biol.* 98:717–724.

33. Taylor, D. L., J. Reidler, J. A. Spudich, and L. Stryer. 1981. Detection of actin assembly by fluorescence energy transfer. *J. Cell Biol.* 89:362–367.

34. Terasaki, M., J. Song, J. R. Wong, M. J. Weiss, and L. B. Chen. 1984. Localization of endoplasmic reticulum in living and glutaraldehyde-fixed cells with fluorescent dyes. *Cell.* 38:101–108.

35. Thomas, D. D., W. F. Carlsen, and L. Stryer. 1978. Fluorescence energy transfer in the rapid-diffusion limit. *Proc. Natl. Acad. Sci. USA.* 75:5746–5750.

36. Tietze, C., P. Schlesinger, and P. Stahl. 1982. Mannose-specific endocytosis receptor of alveolar macrophages: demonstration of two functionally distinct intracellular pools of receptor and their roles in receptor recycling. *J. Cell Biol.* 92:417–424.

37. Tycko, B., and F. R. Maxfield. 1982. Rapid acidification of endocytotic vesicles containing α_2-macroglobulin. *Cell.* 28:643–651.

38. Uster, P. S., and D. W. Deamer. 1981. Fusion competence of phosphatidylserine-containing liposomes quantitatively measured by a fluorescence resonance energy transfer assay. *Arch. Biochem. Biophys.* 209:385–395.

39. Vanderwerf, P., and E. F. Ullman. 1980. Monitoring of phospholipid vesicle fusion by fluorescence energy transfer between membrane-bound dye labels. *Biochim. Biophys. Acta.* 596:302–314.

40. Warburg, O., and W. Christian. 1941. Isolierung und kristallisation des gaerungsferments enolase. *Biochem. Z.* 310:384–421.